

Long-term, induced expression of Hand2 in peripheral sympathetic neurons ameliorates sarcopenia in geriatric mice

Anna Carolina Zaia Rodrigues^{1,2*}, María Laura Messi^{1*}, Zhong-Min Wang^{1*}, Henry Jacob Bonilla¹, Willard M. Freeman³ & Osvaldo Delbono^{1,2,4*} 

¹Department of Internal Medicine, Section on Gerontology and Geriatric Medicine, Wake Forest School of Medicine, Winston-Salem, NC, USA; ²The Neuroscience Program, Wake Forest School of Medicine, Winston-Salem, NC, USA; ³Oklahoma Medical Research Foundation, Oklahoma City, OK, USA; ⁴The Sticht Center for Healthy Aging and Alzheimer's Prevention, Wake Forest School of Medicine, Winston-Salem, NC, USA

Abstract

Background The discovery of adrenoceptors, which mediate the effects of the sympathetic nervous system neurotransmitter norepinephrine on specific tissues, sparked the development of sympathomimetics that have profound influence on skeletal muscle mass. However, chronic administration has serious side effects that preclude their use for muscle-wasting conditions such as sarcopenia, the age-dependent decline in muscle mass, force, and power. Devising interventions that can adjust neurotransmitter release to changing physiological demands will require understanding how the sympathetic nervous system affects muscle motor innervation and muscle mass, which will prevent sarcopenia-associated impaired mobility, falls, institutionalization, co-morbidity, and premature death. Here, we tested the hypothesis that prolonged *heart and neural crest derivative 2* (Hand2) expression in peripheral sympathetic neurons (SNs) ameliorates sympathetic muscle denervation, motor denervation, and sarcopenia in geriatric mice.

Methods We delivered either a viral vector encoding the transcription factor Hand2 or an empty vector (EV) driven to SNs by the PRSx8 promoter by injecting the saphenous vein in 16-month-old C57BL/6 mice that were sacrificed 10–11 months later. Studies relied on sympathetic and muscle immunohistochemistry analysed by confocal microscopy, nerve and muscle protein expression assessed by immunoblots, nerve-evoked and muscle-evoked maximal muscle contraction force, extensor digitorum longus (EDL) muscle RNA sequencing, SN real-time PCR, and tests of physical performance using an inverted-cling grip test and in an open-arena setting.

Results Examining the mice 10–11 months later, we found that inducing Hand2 expression in peripheral SNs preserved (i) the number of neurons (EV: $0.32 \pm 0.03/\mu\text{m}^2$, $n = 6$; Hand2: $0.92 \pm 0.08/\mu\text{m}^2$, $n = 7$; $P < 0.0001$) and size (EV: $279 \pm 18 \mu\text{m}^2$, $n = 6$; Hand2: $396 \pm 18 \mu\text{m}^2$, $n = 7$; $P < 0.0001$); (ii) lumbricalis muscle sympathetic innervation (EV: $1.4 \pm 1.5 \mu\text{m}/\mu\text{m}^2$, $n = 5$; Hand2: $12 \pm 1.8 \mu\text{m}/\mu\text{m}^2$, $n = 5$; $P < 0.001$); (iii) tibialis anterior, gastrocnemius, EDL, and soleus muscles weight and whole-body strength (EV: $48 \pm 6.4 \text{ s}$, $n = 6$; Hand2: $102 \pm 6.8 \text{ s}$, $n = 6$; $P < 0.001$); (iv) EDL type IIb, IIx, and II/IIx and soleus type I, IIa, IIx, IIa/IIx, and IIb/IIx myofibre cross-sectional area; (v) nerve-evoked (EV: $16 \pm 2.7 \text{ mN}$; Hand2: $30 \pm 4.4 \text{ mN}$; $P < 0.001$) and muscle-evoked (EV: $24 \pm 3.8 \text{ mN}$, $n = 5$; Hand2: $38 \pm 3.0 \text{ mN}$, $n = 8$; $P < 0.001$) muscle force by 150 Hz–3 s pulses; and (vi) motor innervation assessed by measuring presynaptic/postsynaptic neuromuscular junction area overlay.

Conclusions Preserving Hand2 expression in SNs from middle-aged to very old mice attenuates decreases in muscle mass and force by (i) maintaining skeletal muscle sympathetic and motor innervation, (ii) improving membrane and total acetylcholine receptor stability and nerve-evoked and muscle-evoked muscle contraction, (iii) preventing the elevation of inflammation and myofibrillar protein degradation markers, and (iv) increasing muscle autophagy.

Keywords Skeletal muscle; Hand2; Neuromuscular junction; Denervation; Atrophy; Sympathetic nervous system; Ageing

Received: 24 February 2021; Revised: 20 July 2021; Accepted: 6 August 2021

*Correspondence to: Osvaldo Delbono, Department of Internal Medicine, Section on Gerontology and Geriatric Medicine, Wake Forest School of Medicine, Medical Center Boulevard, Winston-Salem, NC 27157, USA. Phone: 336-716-9802, Email: odelbono@wakehealth.edu

[†]These authors contributed equally to this work.

Introduction

Age-dependent loss of skeletal muscle mass, strength, and power, termed *sarcopenia*, contributes to disability and impaired quality of life.¹ Of several mechanisms proposed to explain sarcopenia's onset and progression, myofibre motor denervation is identified as a primary culprit.^{1,2} However, therapeutic strategies to prevent or ameliorate sarcopenia are still under investigation. Whether muscle denervation starts at the myofibre or the central or peripheral nervous system is controversial.³ Answering these questions is essential for developing targeted interventions to prevent or reverse age-related decline in skeletal muscle innervation and sarcopenia.

Interventions to preserve muscle mass can improve strength and power in the elderly.⁴ Growing evidence supports diminished neural influence on skeletal muscle at older ages, followed by changes in muscle fibre-type composition, non-homogenous myofibre atrophy, and motor-unit remodelling.³ Although we demonstrated the plasticity of muscle innervation in elderly men and women who practised a resistance training regimen, the benefits were partial, variable, and difficult to sustain for most.⁵ Targeting the mechanisms that drive neuromuscular junction (NMJ) instability and muscle denervation will lead to more effective interventions to prevent or reverse sarcopenia.⁶

Humans undergo symptoms of autonomic nervous failure with ageing.⁷ Autonomic alterations and muscle weakness have been reported in several nervous system disorders and age-associated neurodegenerative diseases. These changes may impair adaptation to common physiological stressors and increase the risk of developing diseases that, in turn, harm autonomic function. Although this observation has been established for organ systems,⁷ the role of the autonomic nervous system in stabilizing the NMJ has been reported only recently in animal models of systemic chemical⁸ or focal surgical ablation of the sympathetic nervous system (SNS), and old, but not geriatric mice.⁹

The discovery of adrenoceptors, which mediate the effects of the SNS neurotransmitter noradrenaline (NA) on specific tissues, ignited the development of sympathomimetics that have profound influence on skeletal muscle mass.¹⁰ However, chronic administration has serious side effects that preclude their use for muscle-wasting conditions like sarcopenia.¹¹ Interventions that can adjust NA release to changing physiological demands depend on understanding how the SNS affects muscle mass and motor innervation across ages.

If sympathomimetic agents enhance NMJ transmission¹² and remediate muscle wasting and strength in aged rodents, why do endogenously secreted catecholamines fail to maintain muscle mass and force in the absence of significant changes in levels of β 2-adrenergic receptors (ARs), which binds adrenaline and NA? Recent studies support a novel mechanism by which motor and sympathetic neurons (SNs) interact at the NMJ presynapse.^{8,9,12} Impaired neuronal crosstalk can explain, at least partially, progressive atrophy and weakness with ageing.

Maintaining or recovering sympathetic muscle innervation throughout life is undoubtedly preferable to chronic use of AR pharmacological agents. Drug administration cannot mimic the complex, concerted tissue response to endogenous SN neurotransmitters, which depends on the AR subtype's repertoire and location. Loss of receptor selectivity, tolerance, and tachyphylaxis can also trigger adverse effects. Moreover, pharmaceutical compounds reach stable levels in blood, precluding any adaptation to physiological or pathological challenges.

We propose that SNs physiologically stabilize motor innervation, preventing sarcopenia. Recently, we found that NA discharge at SN terminals modulates motoneurons' spontaneous and evoked release of synaptic vesicle acetylcholine through the coordinated activity of transient receptor potential cation channels and β 1-AR and α 2B-AR.¹² Our comprehensive approach to examine SNS influence on muscle motor innervation includes nerve immunolabelling co-registration and electrophysiological recordings in a novel mouse *ex vivo* preparation that preserves the complexity of the interaction between motoneurons and the SNS at the NMJ and muscle innervation in living mice. We found that SN regulation of motoneuron synaptic vesicle release, mediated by β 1-AR and α 2B-AR, was blunted in geriatric mice. We propose that age-associated sympathetic hyperactivity explains AR down-regulation at the NMJ presynapse. We have yet to determine whether a decrease in the number of SN also accounts for the decrease in AR expression in geriatric mice.

Recently, we demonstrated that expression of the *heart and neural crest derivative 2* (Hand2), a critical transcription factor for post-mitotic maintenance of SNs,¹³ declines over time, but inducing its expression in old mice preserves (i) the number and size of SNs; (ii) muscle sympathetic innervation; (iii) muscle weight and force and whole-body strength; (iv) myofibre size, but not muscle fibre-type composition; (v) NMJ transmission and nerve-evoked muscle force; and (vi) motor innervation. Because the SNS controls a set of

genes to reduce inflammation and to promote transcription factor activity, cell signalling, and synapse in the skeletal muscle, we also tested whether Hand2 expression would prevent or ameliorate sarcopenia in mice aged 26–27 months, equivalent to human age 75.¹⁴

The study reported here was designed to determine whether Hand2 expression in peripheral SNs for almost half of the mouse life is beneficial in very old age. Specifically, we tested the possibility that inducing Hand2 expression exclusively in SNs for about a year would significantly attenuate (i) motor denervation, (ii) impaired nerve-evoked muscle contraction, and (iii) loss of muscle mass and function when the mice became geriatric.

Material and methods

Animals and ethics statement

Middle-aged (16-month-old) male and female C57BL/6 mice were obtained from the National Institute on Aging and housed in the pathogen-free Animal Research Program of the Wake Forest School of Medicine. After viral vector injections at 16 months, mice were maintained at 21°C and a 12:12 h dark/light cycle for 10–11 months and euthanized at 26–27 months. All mice were fed with chow *ad libitum* and had continuous access to drinking water. All experimental procedures were conducted in compliance with National Institutes of Health laboratory animal care guidelines. We made every effort to minimize their suffering. The Wake Forest School of Medicine Institutional Animal Care and Use Committee approved Protocols A15-219 and A-18-204 for this study.

Statistical analysis

All experiments and analyses were conducted blind to treatment group. No statistical methods were used to predetermine sample sizes; however, our sample sizes are similar to those reported in recently published studies.¹⁵ SigmaPlot Version 12.5 (Systat Software, Inc., San Jose, CA) and Microsoft Excel software were used for statistical analyses. All data were expressed as mean \pm standard error of the mean. Student's *t*-test was used to compare two groups, and analysis of variance followed by Bonferroni's *post hoc* analysis was used to compare three or more. An analysis of variance repeated measures test was used to compare means across one or more variables based on repeated observations. The figure legends indicate the specific tests for each set of experiments. A *P*-value <0.05 was considered significant.

Material and methods for (i) skeletal muscle histochemical and immunofluorescence analyses, (ii) whole-mount

lumbricalis muscle immunohistochemistry and confocal imaging, (iii) paravertebral sympathetic ganglia immunohistochemistry and confocal imaging, (iv) neurofilament (NF) or TH+ path length and NMJ co-localization analysis in confocal images, (v) assessment of muscle force generated by direct muscle-evoked or nerve-evoked stimulation, (vi) protein isolation and immunoblots, (vii) inverted grip test, (viii) spontaneous locomotor activity, (ix) real-time quantitative PCR, (x) viral vector constructs, (xi) viral vector delivery, and (xii) RNA sequencing are in Material and Methods in the Supporting Information.

Results

Induced Hand2 expression preserves the number and size of paravertebral sympathetic ganglia neurons. We previously measured Hand2 mRNA by quantitative real-time PCR through the entire C57BL/6 mouse lifespan.

Transcript levels drop $>50\%$ from Postnatal Day 5 (P5) to 16 months and further decline to become undetectable in geriatric mice.¹⁵ We use P5 as a reference because it marks the highest postnatal expression of *Hand2* in sympathetic ganglia. This approach allows us to compare the decline in Hand2 levels between any two age points. *Hand2* mRNA levels decline more than 70% at 26–27 months of age relative to P5.¹⁵ We previously showed immunoreactivity to a Hand2 antibody in sympathetic ganglion neurons from Hand2-treated, but not empty vector (EV)-treated 22-month-old mice.¹⁵ This approach allowed us to determine that $91 \pm 4.5\%$ of the neurons from Hand2-treated geriatric mice ($n = 5$) show detectable levels of nuclear Hand2 protein.

To determine whether sustaining Hand2 levels in SNs preserve their number and soma area, we systemically delivered a viral vector carrying Hand2 expression (ITR-CAG-EGFP-PRSX8-Hand2-WPRE-ITR-serotype 9) or an EV (ITR-CAG-EGFP-PRSX8-WPRE-ITR-serotype 9) by saphenous vein injection in 16-month-old mice that were sacrificed 10–11 months later.

Confocal images of ganglia neurons from EV-treated and Hand2-treated mice (*Figure 1*) show that they are tyrosine hydroxylase positive (TH+; red) with nucleus staining (Hoechst, blue). However, the Hand2-treated mice have more ganglia neurons with larger soma size (B) than the EV-treated mice (A), which we could determine because we analysed the entire individual ganglion. Note that ganglia from EV-treated mice show areas devoid of TH+ neurons.

These results indicate that sustained Hand2 expression in paravertebral SNs prevents their loss and atrophy in geriatric mice, consistent with a very significant increase in *Hand2* mRNA levels in the Hand2-treated compared with EV-treated mice (C), the number of TH+ neuron per ganglion area (D), and TH+ neuron size (E).

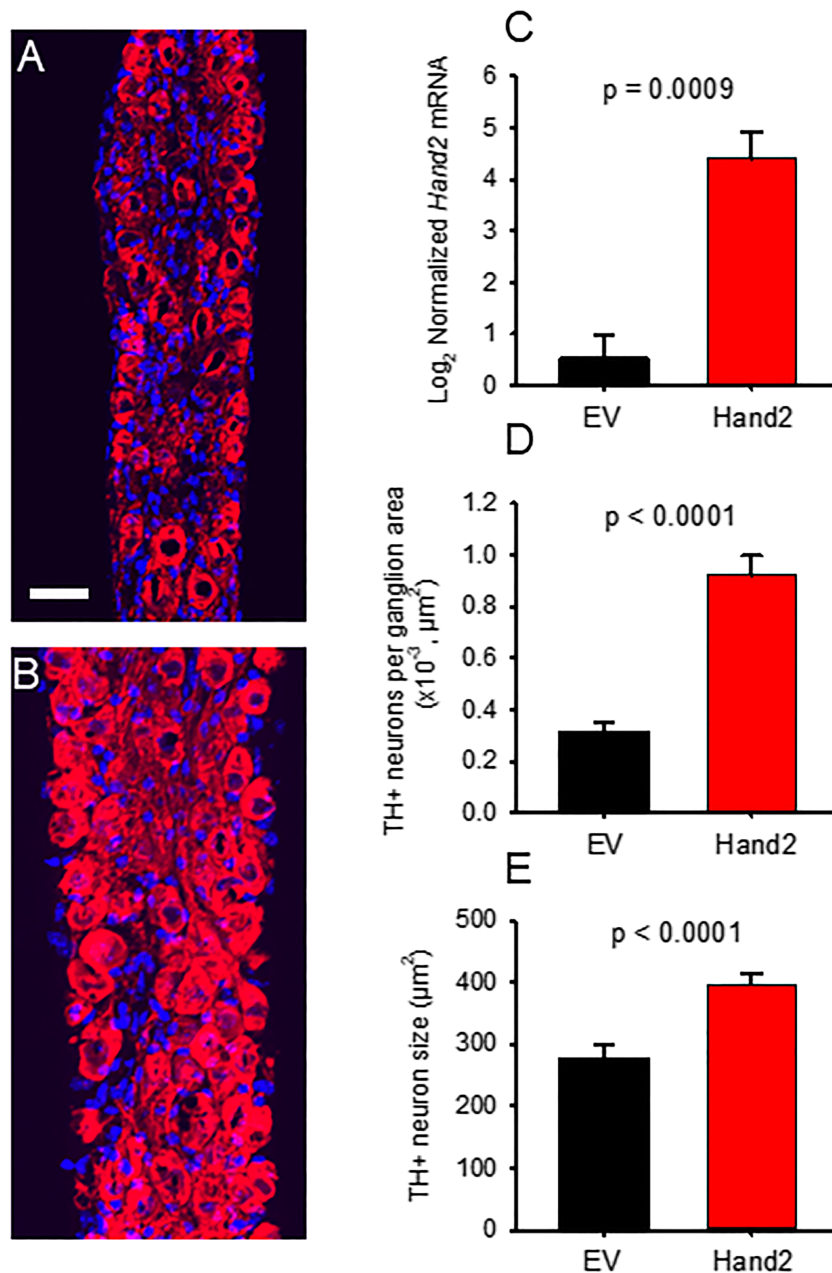


Figure 1 *Hand2* mRNA preserves sympathetic neuron number and size into old age. EV-treated (A) and Hand2-treated (B) mice show TH+ neurons (red) and nucleus staining (blue). Calibration bar = 50 μm. Compared with the EV group, ganglia neurons from the Hand2-treated mice show significantly higher *Hand2* mRNA levels ($n = 7$ ganglia from 7 EV-treated mice and 10 ganglia from 10 Hand2-treated mice) (C); more TH+ neurons ($n = 6$ ganglia confocal images from 6 EV-treated mice and 7 ganglia from 5 Hand2-treated mice) (D); and larger TH+ neurons ($n = 6$ ganglia confocal images from 6 EV-treated mice and 7 ganglia from 5 Hand2-treated mice) (E). Data in (C)–(E) were statistically analysed by non-paired *t*-test.

Sympathetic neuron heart and neural crest derivative 2 attenuates loss in muscle weight and force and whole-body strength in geriatric mice

Figure S1 shows that compared with EV treatment, Hand2 treatment significantly attenuates loss in fast [tibialis anterior (TA) and extensor digitorum longus (EDL) muscle] (A, C), and mixed fibre-type [gastrocnemius (GA) and soleus] (B, D)

muscles, and muscle weight. Body (E), heart (F), and visceral fat (G) weight did not differ significantly between treatment groups. Figure S2 shows that spontaneous mobility—tested as spontaneous maximum speed (A), average speed (B), total distance travelled (C), and time spent in motion (D) in an open-arena setting—did not differ significantly. However, compared with EV treatment, Hand2 treatment significantly attenuated loss in net-hanging time, a measure of muscle

strength (E). These results indicate that sustained Hand2 expression in SNs significantly prevents skeletal muscle weight and force and whole-body strength in geriatric mice.

Preserved sympathetic neuron heart and neural crest derivative 2 expression attenuates myofibre atrophy but does not modify muscle fibre-type composition

To determine whether preserved lean mass accounts for the improvement in muscle weight and force, we quantified myofibre number and cross-sectional area (CSA) in muscle transversal cuts stained with antibodies specific for myosin heavy chain (MyHC) subtypes. We selected EDL and soleus muscles because of their highly predominant type II and I/II fibre composition, respectively, and total muscle CSA because it can be fully quantified. *Figure 2* shows no differential effects between muscle fibre types (A–F), but in both, some fibres' CSA was maintained (A–D, G, H). Specifically, the CSA of EDL type IIb, IIx, and IIb/IIx (G) and soleus type I, IIa, IIx, IIb/IIx, and Ib/IIx (H) fibres was preserved significantly in Hand2-treated but not EV-treated mice. These results indicate that preserving sympathetic innervation significantly ameliorates age-related muscle atrophy.

Sustained heart and neural crest derivative 2 expression in sympathetic neurons stabilizes membrane acetylcholine receptor, regulates neuromuscular junction preterminal adrenoceptors, and prevents loss of nerve-evoked muscle force

To investigate whether attenuating muscle sympathetic denervation stabilizes acetylcholine receptor (AChR) and regulates preterminal AR levels, we measured both groups of receptors by immunoblot. *Figure 3* shows that Hand2 enhances both membrane (A–C) and total (D–F) AChR levels in GA and TA muscles as well as AR levels in presynaptic β 1-adrenergic (G, H) and α 2B-adrenergic (I, J) but not postsynaptic β 2-adrenergic (K–M) receptors.

To determine whether improved neuromuscular transmission affects the generation of muscle force, we measured nerve-evoked muscle contraction at increasing frequencies (2–150 Hz) in EV-treated and Hand2-treated mice using the same preparation.⁹ We elicited lumbricalis muscle contraction by plantar nerve stimulation and then blocked neuromuscular transmission with 10^{-5} g/mL D-tubocurarine. After verifying that nerve stimulation did not evoke muscle contraction, we switched to direct muscle stimulation, applying field pulses and repeat maximal specific sub-tetanic and tetanic force at the same frequencies. *Figure 4Aa* shows that the tetanic force in response to 100 Hz pulses applied for 1 s

to the distal peroneal nerve near the lumbricalis muscle was not sustained and reached a lower peak in EV-treated (black trace) than Hand2-treated (red trace) mice. Single twitches recorded in these muscles also showed less force in the EV group (Ab). Differences between the groups were significant at all frequencies except 5 Hz (C). Tetanic force developed in response to direct stimulation of lumbricalis muscle had a lower peak and weaker twitches in EV-treated than Hand2-treated mice (Ba, b). For this effect, differences between groups were significant at all frequencies (D).

These results indicate that sustained Hand2 expression in SNs preserves NMJ transmission, muscle innervation, and muscle-evoked and nerve-evoked muscle contraction.

Heart and neural crest derivative 2 attenuates neuromuscular junction post-terminal motor denervation

We investigated whether SN Hand2 attenuates the muscle denervation seen with ageing. *Figure 5* compares muscle areas of the same dimensions enriched in NMJs. EV-treated geriatric mice show a mixture of innervated (white arrows) and denervated (yellow arrows) terminals (A), but in those treated with Hand2, more are innervated and fewer denervated than in the EV group (B). To quantify the difference, we detected NMJ innervation with antibodies against either non-phosphorylated (SMI 311) or phosphorylated (SMI 312) NF and analysed preterminal and post-terminal NMJ co-localization using the Pearson correlation coefficient (C), Spearman's rank correlation coefficient (D), and Manders' co-localization coefficient M1 (E). The analysis shows that Hand2-treated mice preserve innervation significantly more than the EV group.

To further investigate the mechanism underlying differences in NMJ innervation, we measured the total NF + path length normalized to muscle area. The difference was not significant for non-phosphorylated NF but significant for phosphorylated NF (*Figure 5F*). In the Hand2-treated mice, phosphorylation of the three NF subunits—heavy (NFH, *Figure S3A*), medium (NFM, *Figure S3B*), and light (NFL, *Figure S3C*)—was greater than in the EV-treated mice, consistent with the analysis of NMJ innervation (*Figure 5*) and possibly explained by the significant decrease in phosphatases PP2A (*Figure S3D*) and PP1 (*Figure S3E*). These results indicate that sustained Hand2 expression in SNs attenuates myofibre denervation and NF dephosphorylation in geriatric mice.

Heart and neural crest derivative 2 attenuates muscle sympathetic denervation with ageing

Figure 6 shows NMJ post-terminals (blue) and sympathetic axons surrounding blood vessels (arrows) (green) located far from the post-terminals with no overlap in EV-treated

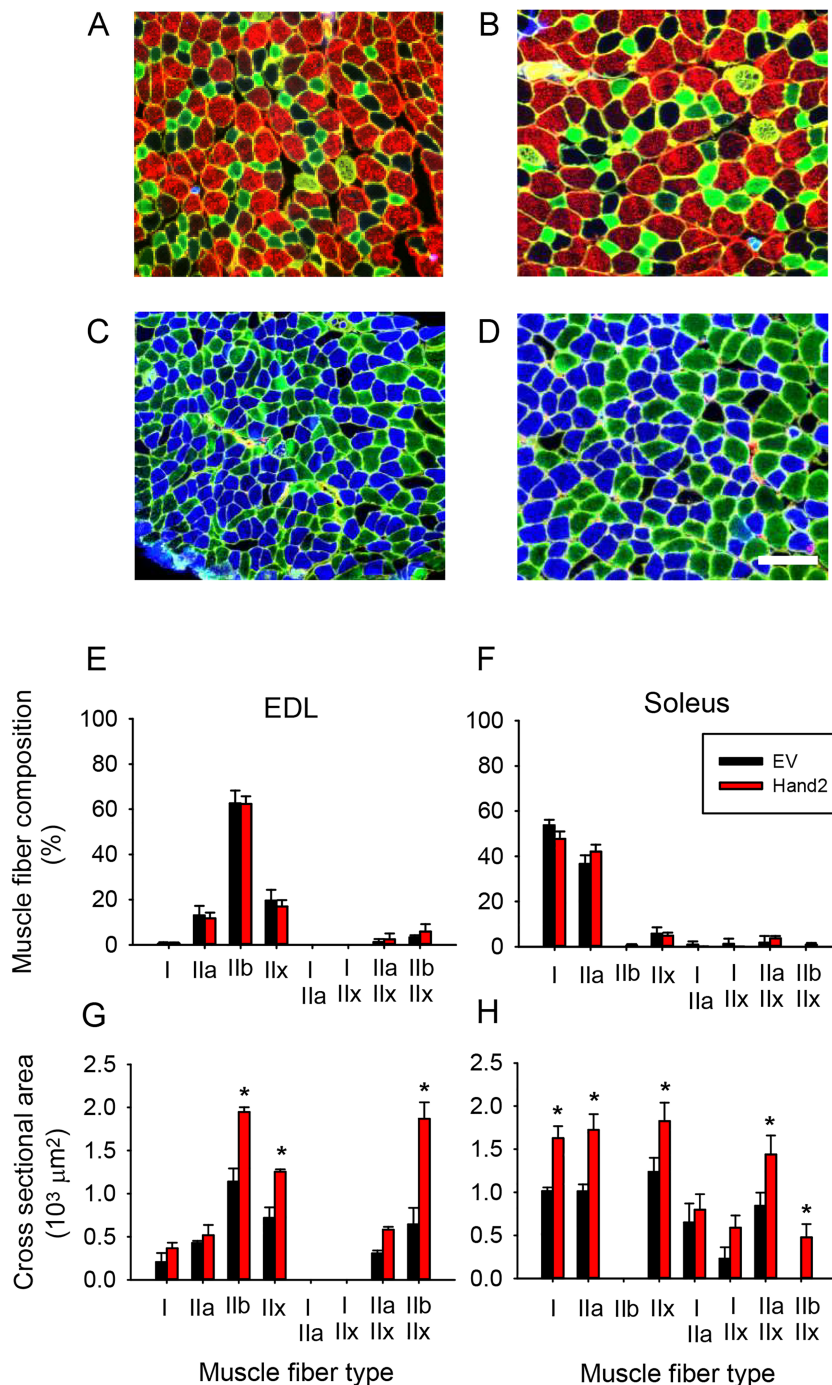


Figure 2 Hand2 expression in sympathetic neurons attenuates age-dependent muscle atrophy as assessed by histological MyHC immunofluorescence. (A, B) Compared with EV-treated mice (A, C), Hand2-treated mice have larger EDL (B) and soleus (D) muscle cross-sections. Myofibres were immunostained with specific MyHC antibodies to identify type I (blue secondary Ab), type IIa (green), and type IIb (red) fibres. Fibres negative to these three antibodies were labelled type IIx. Calibration bar = 50 μm. EDL (E) and soleus (F) pure and hybrid muscle fibre composition, expressed as a per cent of the total number of fibres, did not differ significantly between groups. In contrast, muscle fibre cross-sectional area showed statistically significant between-group differences in EDL for type IIb ($P = 3.5e^{-4}$), IIx ($P = 0.001$), and IIb + IIx ($P = 0.7e^{-4}$) fibres (G) and soleus for type I ($P = 0.001$), IIa ($P = 0.004$), IIx ($P = 0.045$), IIa/IIx ($P = 0.041$), and IIb + IIx ($P = 0.008$) fibres (H). $N = 10$ EDL or soleus muscles from six mice per group. Values were averaged when two muscles from a single mouse were used. Data were compared using one-way ANOVA.

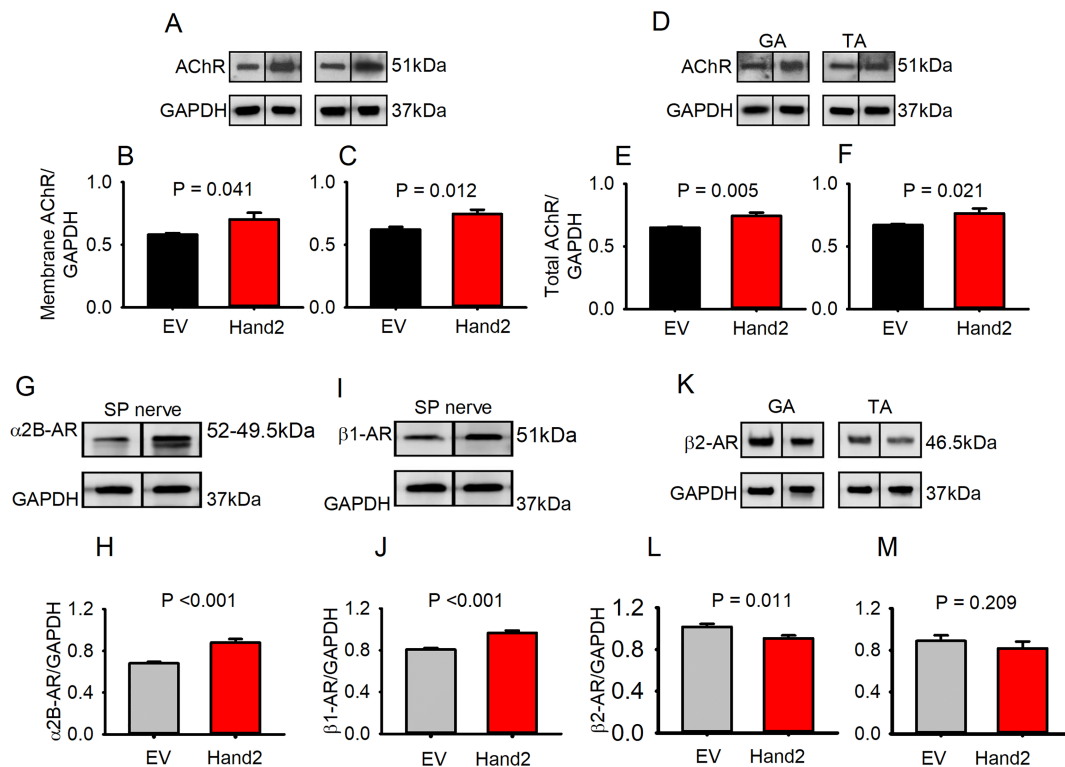


Figure 3 Sustained Hand2 expression in sympathetic neurons prevents decline in AChR levels and presynaptic β 1-adrenergic and α 2B-adrenergic receptors with ageing. Immunoblot analysis of membrane (A) and total (D) AChR in GA and TA muscles from the EV group ($n = 8$ GA and 8 TA muscles from six different mice) and the Hand2 group ($n = 8$ GA and 8 TA muscles from six different mice). The digital optical density of the bands was normalized to GAPDH and is quantified in graphs (B), (C), (E), and (F), respectively. Using a similar approach, sciatic–peroneal (SP) β 1-AR (G, H) and α 2B-AR (I, J) were higher, but muscle β 2 (K–M) showed no significant changes between groups with ageing. $N = 8$ nerves or muscles from an equal number of mice per treatment group. Data were statistically analysed using a non-paired *t*-test.

geriatric mice (A). In contrast, Hand2-treated mice show richer, more complex muscle sympathetic innervation than the EV group (B). Sympathetic axons overlap with several NMJ post-terminals (yellow arrows). Immunoblot shows that TH levels are higher in the sciatic–peroneal nerve from Hand2-treated than from EV-treated mice (C, E). Similarly, GA and TA muscles show higher TH levels in Hand2-treated mice (D, F, G). We also determined that Hand2 expression significantly decreased the distance between sympathetic terminals and NMJs (H), while significantly preserving the density of sympathetic terminals per muscle area (I). These results indicate that sustained Hand2 expression in SNs supports the complexity of muscle sympathetic innervation and its relationship with NMJs in geriatric mice.

Sustained sympathetic neuron Hand2 expression prevents activation of the myofibre $G\alpha_{i2}$ -Hdac4-myogenin–MyoD–atrogin/MuRF1 signalling cascade

Figure S4 shows that Hand2 maintains higher levels of the inhibitory G-protein $G\alpha_{i2}$ (A–C), which leads to lower Hdac4

(D–F), myogenin (G–I), MyoD (J–L), atrogin (M–O), and MuRF1 (P–R) levels, as tested by immunoblot in GA and TA muscles. These results indicate that Hand2 prevents activation of a signalling pathway previously shown to be triggered by ablation of skeletal muscle sympathetic innervation.⁹

Sympathetic heart and neural crest derivative 2 expression preserves protein kinase A regulatory subunit I and Akt phosphorylation

Figure S5 shows more PKA RI (A, B), less PKA RII (C, D), a lower PKA/RII/PKA RI ratio (E), and significant Akt phosphorylation in both muscles from mice treated with Hand2 (F, G). Although the GA muscle showed higher PKA RI levels, the difference was not significant, but the decrease in PKA RII and the lower PKA RII/RI ratio were significant in both muscles. These findings indicate that (i) chronic Hand2 treatment activates canonical and non-canonical β -AR signalling and (ii) sympathetic Hand2 expression counters the age-associated decrease in PKA RI, sustains RII-subunit levels, and lowers the PKA/RII/PKA RI ratio, which may influence AChR stability and myofibre innervation.¹⁶

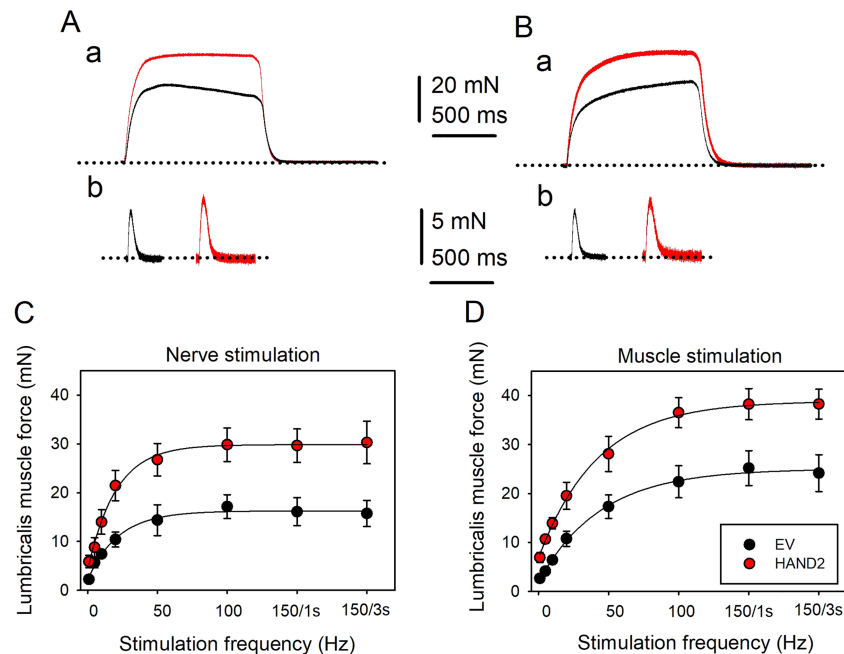


Figure 4 Hand2 treatment preserves muscle force in response to single or repetitive nerve or muscle stimulation in geriatric mice. (Aa) Tetanic force developed in response to 100 Hz pulses applied for 1 s to the distal peroneal nerve near the lumbricalis muscle from a Hand2-treated (red) or EV-treated (black) mouse. (Ab) Single twitches recorded in the muscles tested in (Aa). Dotted lines represent the baselines. (Ba) Tetanic force developed in response to 100 Hz pulses applied for 1 s to the lumbricalis muscle from a Hand2-treated (red) or EV-treated (black) mouse. (Bb) Single twitches recorded in the muscles tested in (Ba). (C) Lumbricalis muscle force in millinewtons (mN) as a function of distal peroneal stimulation at increasing frequency (1–150 Hz). Differences between Hand2-treated (red symbols) and EV-treated (black symbols) mice at 1, 5, 10, 20, 50, 100, 150–1 s, and 150–3 s are (mean \pm SEM), P -values: 0.026, 0.09, 0.026, 0.006, 0.018, 0.009, 0.009, and 0.013, respectively. (D) Lumbricalis muscle force as a function of direct stimulation at increasing frequencies. $N = 5$ muscles from five EV-treated and eight muscles from eight Hand2-treated mice. Differences between Hand2-treated and EV-treated mice at 1, 5, 10, 20, 50, 100, 150–1 s, and 150–3 s frequencies were (mean \pm SEM), P -values: 0.003, $3e^{-5}$, $5e^{-5}$, 0.015, 0.025, 0.007, 0.016, and 0.011, respectively. Data in (C) and (D) were statistically analysed using ANOVA repeated measures tests.

Heart and neural crest derivative 2 evokes mechanistic target of rapamycin complex 1 and forkhead box O1 phosphorylation but nuclear factor kappa-light-chain-enhancer of activated B cells down-regulation in geriatric mice

Figure S6A and S6B shows that compared with EV treatment, Hand2 treatment showed higher mTORC1 phosphorylation levels at serine 2448, which is independent of Akt activity. However, both kinases might affect atrogin and MuRF1 levels and autophagy (see the succeeding text). Also, FoXO1 (C, D) but not FoXO3 (E, F) phosphorylation remains elevated with Hand2 treatment.

Lower NF- κ B (G, H) and I κ B (I, J) phosphorylation in Hand2-treated mice indicates that sustained skeletal muscle sympathetic innervation prevents NF- κ B–I κ B complex dissociation and NF- κ B shift to the nucleus, preventing the transcription of genes encoding proteins involved in inflammation signalling.

Macroautophagy and chaperone-mediated autophagy

Figure S7 shows that, compared with EV treatment, Hand2 treatment enhances use of p62 (A, B) and the conversion of LC3-I to LC3-II (C, D) in GA and TA muscles. Preserved autophagy flux is associated with higher Atg7 levels in both muscles (E, F). Analysis of changes in a key component of the chaperone-mediated autophagy (CMA) pathway, such as the heat shock cognate 70 kDa protein (G, H), showed no significant differences between treatment groups.

Sustained heart and neural crest derivative 2 sympathetic neuron expression in old mice regulates the skeletal muscle transcriptome

Previous work shows that SNS ablation extensively changes the skeletal muscle transcriptome.⁹ Figure 7A–7D shows that Hand2 significantly regulates skeletal muscle genes, as

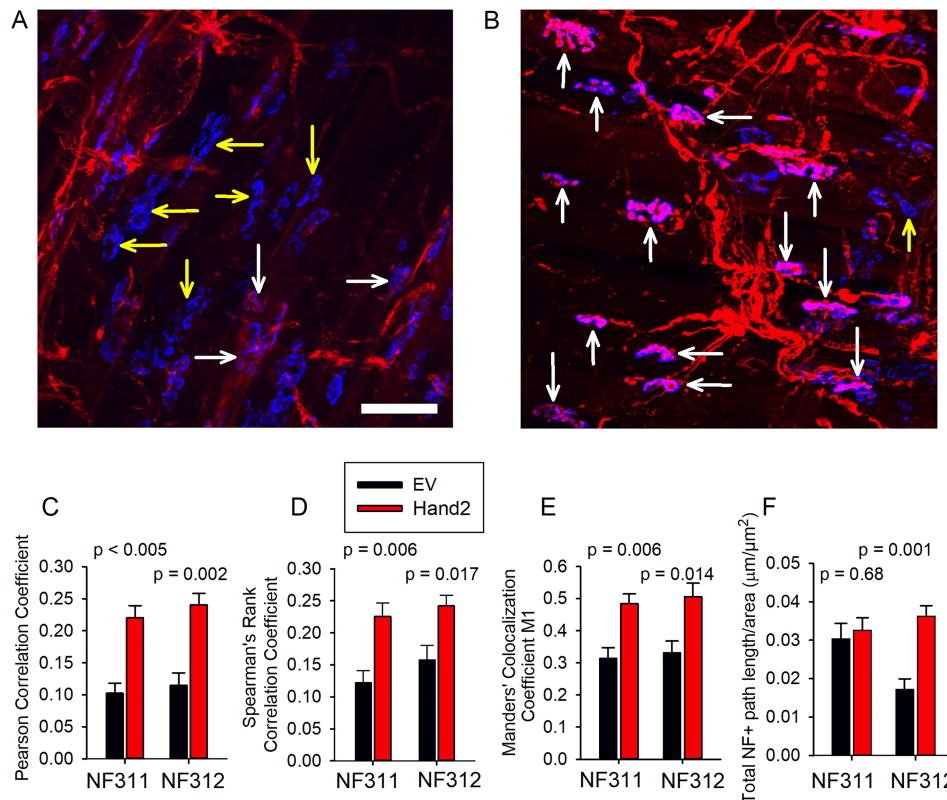


Figure 5 Sympathetic neuron Hand2 attenuates motor denervation in lumbricalis muscle fibres from geriatric mice. Z-stack confocal images of NMJs from 27-month-old EV-treated (A) and Hand2-treated (B) mice. The post-terminal (blue) was stained with alpha-bungarotoxin (BGT)-680, and the preterminal was immunostained with the SMI-311 Ab against NF (red). (A) and (B) show preterminal and post-terminal NMJ co-localization in pink (white arrows) and lack of overlay in blue (yellow arrows). Calibration = 50 μm. Preterminal and post-terminal NMJ co-localization in muscles from EV-treated or Hand2-treated mice analysed by Pearson correlation coefficient (C), Spearman's rank correlation coefficient (D), and Mander's co-localization coefficient M1 (E). $N = 10$ muscles per treatment (5 immunostained with SMI 311 and 5 with SMI 312 antibodies). Total and phosphorylated NF paths per muscle area (F).

quantified by RNA sequencing. Individual mouse values are listed in *Table S2*. Hand2 treatment significantly up-regulates rather than down-regulates genes. The functional enrichment analysis of differentially expressed transcripts shows that Hand2 regulates genes encoding critical components of the NMJ and myofibre innervation such as those involved in synaptogenesis, adenylate cyclase, cAMP, G protein-coupled receptors, and CREB signalling pathways (E).

The SNS controls the up-regulation or down-regulation of a combination of genes to reduce inflammation and to promote transcription factor activity, cell signalling, and synapse in the skeletal muscle. Hand2 induced down-regulation of the *cytokine receptor-like factor 1 (clf1)* and *chemokine-like receptor 1 (cmklr1)*, which play a role in preventing the action of pro-inflammatory cytokines in age-related central sympathetic hyperactivity. We have previously related central noradrenergic neurons hyperactivity to the down-regulation of presynaptic adrenoceptors.^{15,17,18} Hand2 also down-regulates *neurexin-2 (nrxn2)*, which is associated with inflammatory pain perception, and *ephrin A2 (efna2)*, which increases neural progenitor cell proliferation. Down-regulation of the *arrestin β2* gene (*arrb2*) may lead to β-AR activation.

Hand2 treatment attenuates age-dependent decreases in *small mothers against decapentaplegic (Smad1)* gene expression, which mediates bone morphogenetic proteins (BMPs), consistent with *insulin-like growth factor-binding protein-3 (IGF2BP3)*-mediated inactivation of transforming growth factor-β signalling. Because BMPs are members of the transforming growth factor-β family, increased *IGF2BP3* is expected to up-regulate *Smad1*. Compared with EV-treated mice, Hand2-treated mice show more *growth arrest and DNA damage inducible beta (Gadd45b)*, which mediates NF-κB suppression of JNK signalling by targeting MKK7/JNKK2.¹⁹

Neuronal activity-induced *Gadd45b* promotes epigenetic DNA demethylation and adult neurogenesis. *Synuclein, alpha interacting protein (SNCAIP, synphillin)* encodes a protein that has several interaction domains, including ankyrin-like repeats that mediate the attachment of membrane proteins to the membrane cytoskeleton. - *G protein subunit alpha L (gnal)*, which is related to the adenylate cyclase inhibitory pathway and DAG and IP3 signalling,²⁰ while *G protein-coupled receptor associated sorting protein 2 (Grasp2)* plays a role in regulating a variety of G protein-coupled receptors.

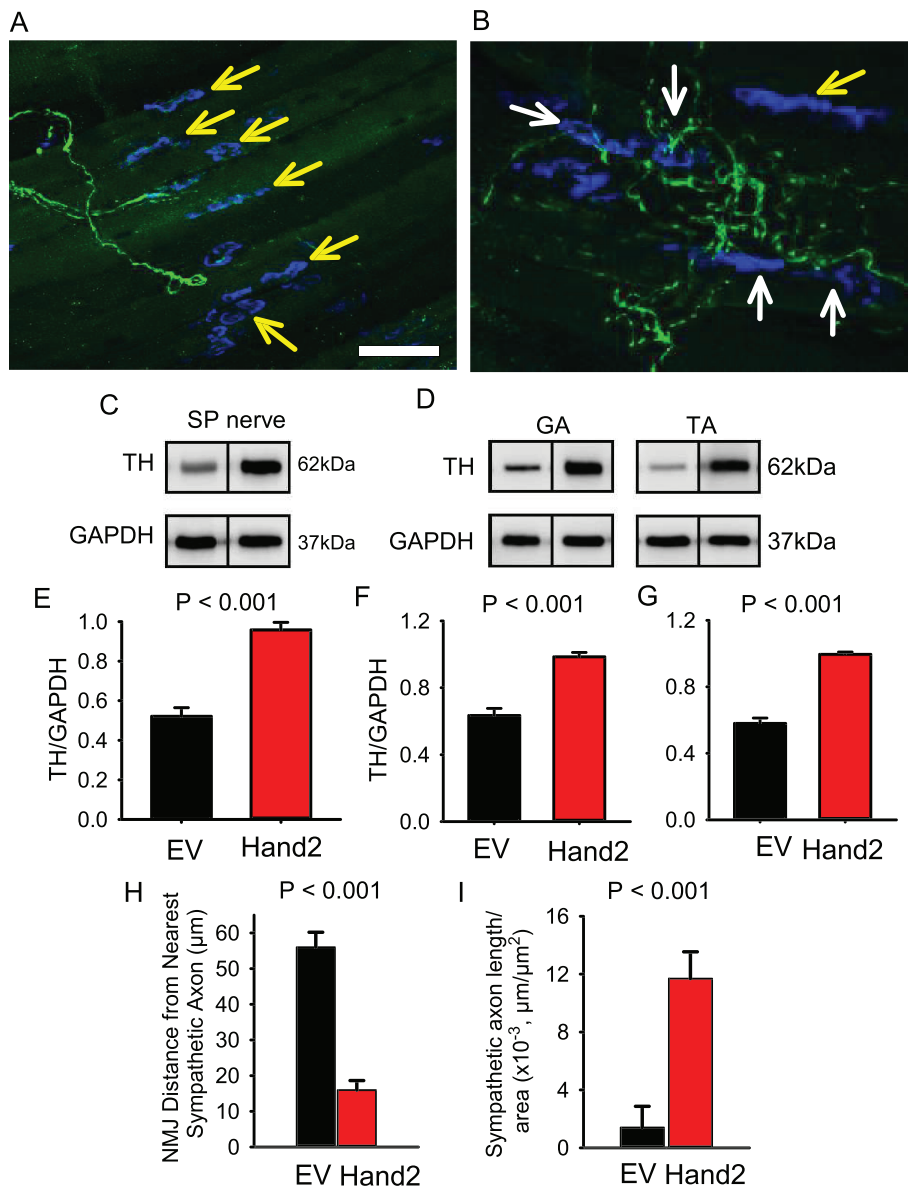


Figure 6 Sympathetic neuron Hand2 preserves the complexity of muscle sympathetic innervation and its proximity to the NMJ. A Z-stack confocal image of a whole-mounted lumbricalis muscle from an EV-treated (A) and a Hand2-treated (B) mouse. Yellow arrows indicate sympathetic axons that do not establish contact with NMJs, while the white arrows show their interaction. Immunoblot analysis shows that Hand2 expression elevates TH expression in the SP sciatic nerve (C) and GA and TA muscles (D–G) in geriatric mice. (H) $N = 8$ lumbricalis, sciatic–peroneal (SP) nerves, GA, or TA muscles from eight different mice per treatment group. In the Hand2 mice, NMJ distance from the nearest sympathetic axon was shorter, and the sympathetic axon path, normalized to the muscle cross-sectional area, was longer ($n = 5$ lumbricalis from five different mice per treatment group) (I). Data were statistically analysed using a non-paired *t*-test.

Discussion

This study shows that selective expression of Hand2 in the mouse peripheral sympathetic system from middle through very old age ameliorates sarcopenia by (i) regulating skeletal muscle sympathetic and motor innervation, (ii) improving AChR stability and nerve-activated muscle force generation, (iii) inhibiting an increase in inflammation markers, (iv) preserving autophagy, and (v) probably attenuating protein degradation by precluding MuRF1 and MAFbx up-regulation (Figure 8).

Inducing heart and neural crest derivative 2 expression preserves the number and size of paravertebral sympathetic ganglia neurons even at advanced ages

Hand2 plays a critical role in adult SNS' maintenance of NA genes²¹ and cell survival as demonstrated by postganglionic sympathetic nerve axotomy experiments and conditional Hand2 KO in SNSs.¹³ Adult nerve injury suppresses Hand2, which directly regulates dopamine beta-hydroxylase (Ddh)

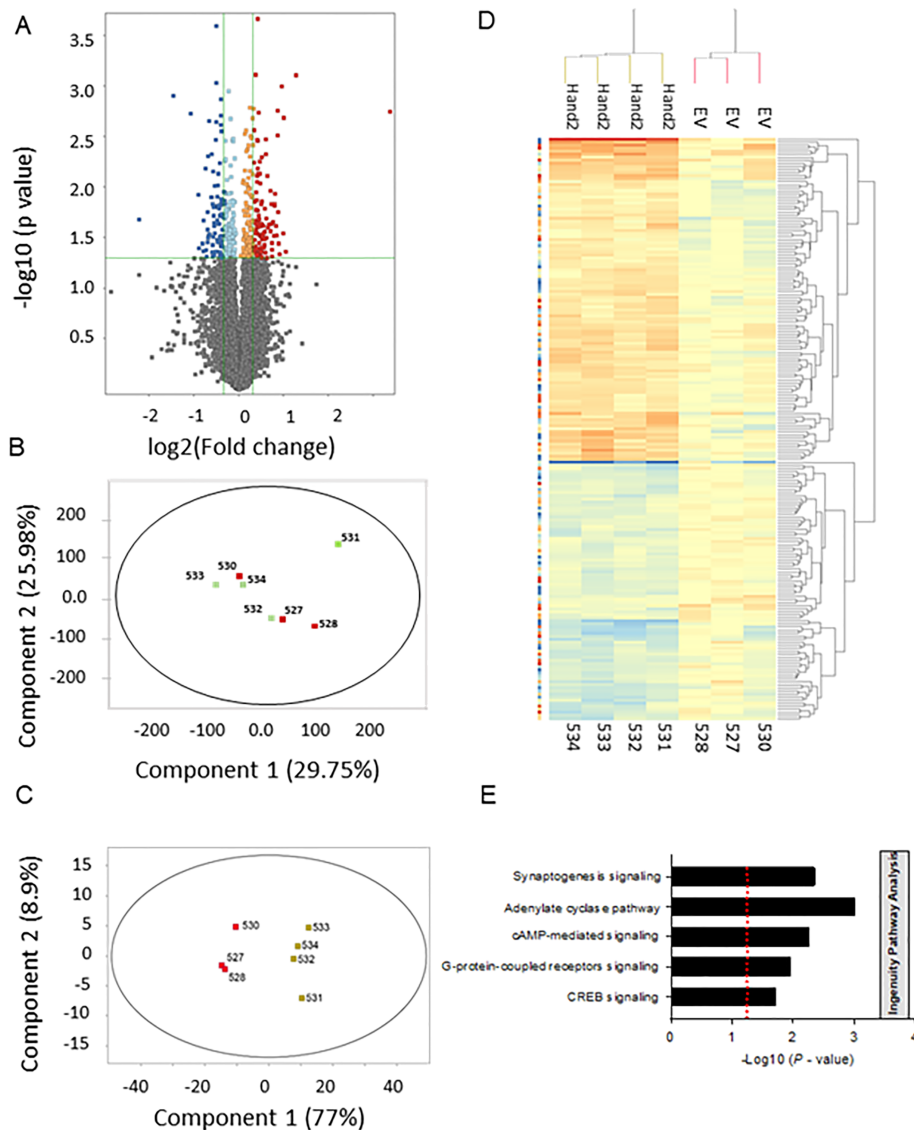


Figure 7 Sustained sympathetic neuron Hand2 expression regulates EDL muscle gene transcription in old mice. (A) Volcano plot representing the significance ($-\log_{10} P$ -value) and magnitude of transcript change (\log_2 fold change) with Hand2 treatment. Some segregation, but not a large separation of Hand2-treated and EV-treated mouse groups by PCA1 or PCA2, is observed when all expressed genes were included in the analysis (B). However, PCA based only on differentially expressed genes shows a clear separation of the two groups (C). (D) Heat map of 191 differentially expressed genes in the EDL muscle from EV-treated ($n = 3$ muscles from three mice) and Hand2-treated ($n = 4$ muscles from four mice) mice. Genes reaching a cut-off significance level of $P < 0.01$ were up-regulated (top 106 genes) or down-regulated (bottom 85 genes). Red and blue indicate up-regulated and down-regulated genes, respectively. *Table S2* provides detailed quantification of up-regulated or down-regulated genes per mouse, labelled 527–534 for the PCA and heat map analysis. Using Strand Next-Generation Analysis Software (see Materials and methods), PCA correlates predictors (multicollinearity) to visualize data in a two-dimensional space and captures over 90% of data variance. We considered transcripts with an average read count value of >10 in 100% of the samples in at least one group sufficiently expressed for quantification. Transcripts expressed below this level were excluded as not detected or not expressed because results were close to background and highly variable. Statistical analysis of differential expression relied on the t -test followed by a Benjamini–Hochberg multiple test correction. A fold change $>|1.25|$ cut-off eliminated genes that were statistically significant but unlikely to be biologically significant or orthogonally confirmable due to the very small magnitude of change. The functional enrichment analysis of differentially expressed transcripts shows that Hand2 regulates genes encoding critical components of the NMJ and myofibre innervation (E).

expression and, most important, the genes controlling synaptic and neurotransmission functions in adult SNs.¹³ A recent study also demonstrates that Hand2 expressed in peripheral SNs significantly attenuates skeletal muscle denervation and

sarcopenia in old mice,¹⁵ but whether this treatment is effective at later ages is unknown. The age of the mouse cohort used in the present study corresponds to geriatric individuals who undergo weakness, mobility disability, and a pronounced

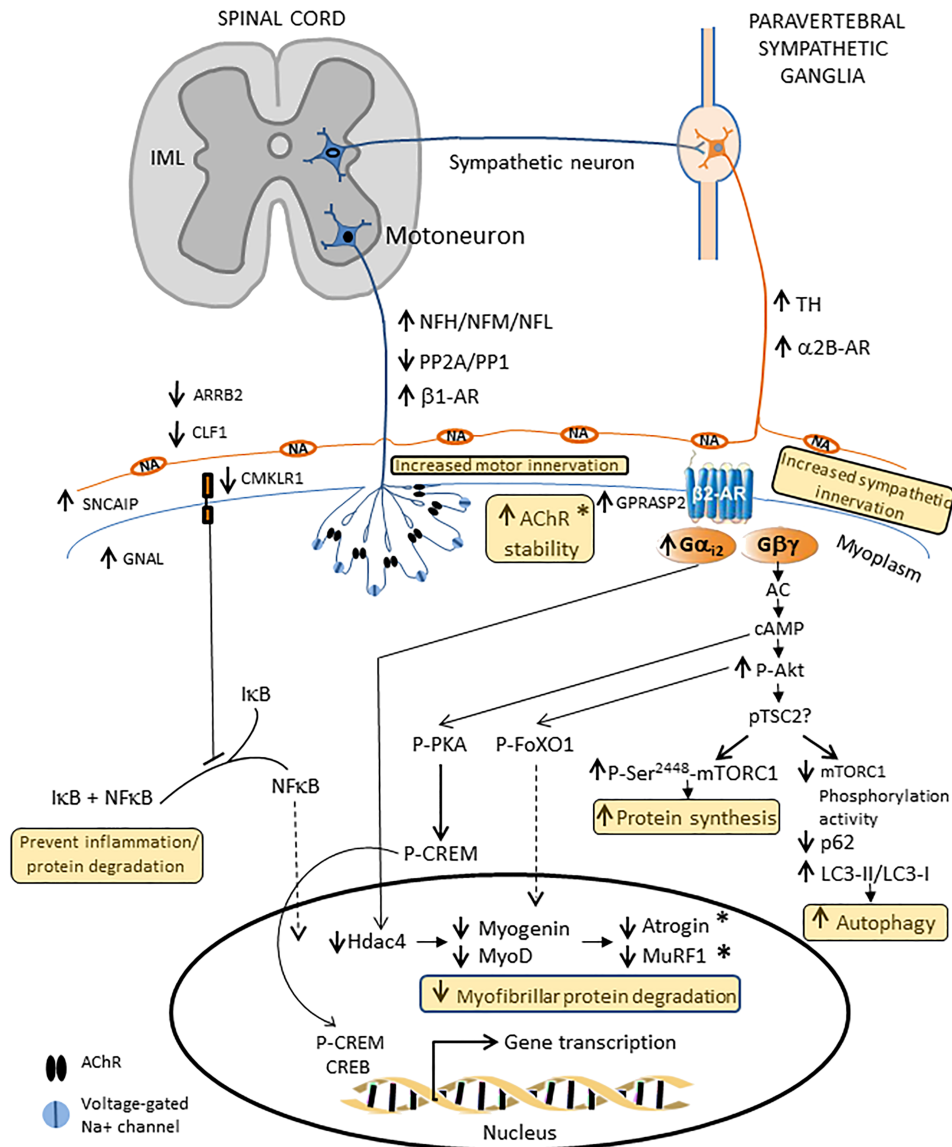


Figure 8 Schematic representation of Hand2-induced expression in SNs and its impact on skeletal muscle sympathetic and motor innervation in geriatric mice. Preserving muscle sympathetic innervation prevents decline in β_2 -AR-associated $G\alpha_{i2}$ and up-regulation of Hdac4, myogenin, MyoD, and MAFbx. Hand2-induced decrease in MuRF1 led to an increase in sarcolemmal AChR. MuRF1 is expressed in both type I and type II fibres, is highly enriched at the post-terminal, and interacts with AChR in endocytic structures.²⁹ Because post-terminal stability has been found crucial to maintaining NMJ structure and myofibre motor innervation,³⁹ we propose that long-term expression of Hand2 in sympathetic neurons preserves muscle motor innervation. MuRF1 is also involved in muscle trophism and maintenance, particularly, by down-regulating thick filaments. β -AR interaction with G-protein $\beta\gamma$ subunits leads to increased P-Ser²⁴⁴⁸-mTORC1, which has been linked to increased protein synthesis. mTORC1 inhibition prevents age-related muscle loss, while its chronic activation advances muscle damage and loss. Autophagy activation is also impaired in ageing skeletal muscle, and its preservation helps to maintain muscle mass in ageing mammals. We propose that, by maintaining sympathetic innervation, Hand2 helps to sustain muscle mass and function in geriatric mice. Hand2-induced, sustained skeletal muscle sympathetic innervation decreases NF- κ B and I κ B levels, which prevents complex dissociation and NF- κ B shift to the nucleus, attenuating the transcription of genes encoding the proteins involved in inflammation signalling, while down-regulation of the *cytokine receptor-like factor 1 (clf1)* and *chemokine-like receptor 1 (cmk1r1)* prevents the action of pro-inflammatory cytokines in age-related sympathetic hyperactivity.

and invalidating reduction in muscle mass.¹ Thus, based on its pivotal role, we focused our research on the impact of Hand2 expression in very old age. Because we restricted its expression to the peripheral SNS,²² we can rule out any influence of central sympathetic relays on our measures.

The reason for the decline in Hand2 expression over time depends, at least partially, on gene hypermethylation. Previous data showed CpG island hypermethylation in paravertebral sympathetic ganglia neurons with ageing.¹⁵ Epigenetic silencing of Hand2 has been reported in

pathologies associated with ageing in humans and rodents.²³

Compared with EV-treated mice, Hand2-treated mice have more ganglia SNs with larger soma size. This difference may be explained by age-dependent neuronal depletion associated with less Hand2 expression.¹³ Conditional deletion of *Hand2* reveals its critical functions in neurogenesis during development²² and adulthood.¹³ Gene delivery to peripheral SNs increased Hand2 mRNA expression several fold compared with that in EV-treated mice as confirmed by RNA sequencing and qPCR. The preservation of SN number, density, and size in Hand2-treated mice extends and enriches the complexity of sympathetic muscle innervation into old age.

Preserved phosphorylated PKA RI and mTORC1 with Hand2 preserve the phosphorylation of the *cAMP-response element binding protein CREB modulator*—CREM, which translocates to the nucleus. Both CREB and CREM bind a specific element—*cAMP-response element* (CRE)—in the promoter region of skeletal muscle target genes.²⁴ Our Ingenuity Pathway Analysis showed that CREM is a top upstream regulator of genes controlled by SNs expressing Hand2 in very old age (P -value = $9.02e^{-8}$). CREM targets include *TH* and *dHand*, two genes essential for SN function and maintenance.²⁵ In summary, low levels of PKA RI phosphorylation,¹⁶ together with genomic hypermethylation, may account for the age-dependent decrease in *Hand2* gene transcription.

Heart and neural crest derivative 2 attenuates loss in skeletal muscle mass and force and whole-body strength but not spontaneous mobility

The body weight of both EV-treated and Hand2-treated mice remained stable, despite attenuated loss in TA, GA, EDL, and soleus muscle mass, with no significant differences in visceral fat or spontaneous activity. We do not know how subcutaneous fat changed with Hand2 treatment and age. Although body fat accumulation has been reported, appendicular, mainly subcutaneous fat declines at later ages, resulting in weight loss.²⁶

The attenuated loss in muscle mass was associated with enhanced muscle strength as shown by the net-hanging time test. We attribute this observation to the preserved CSA of type IIb, IIx, and IIb/IIx fibres in EDL muscle, and type I, IIa, IIx, IIa/IIx, and IIb/IIx fibres in soleus muscle.

Next, we tested force generation in response to electrical stimulation of nerves or muscles using a wide range of frequencies and pulse durations. For these experiments, we used lumbricalis muscle from mouse paws because it has few myofibre layers, which favours oxygenation during prolonged stimulation recording. In addition, its NMJs have banded alignment, and its tendons are arranged in parallel.¹² Distal peroneal nerve stimulation resulted in unsustainable and

weaker peak force than that elicited by direct muscle stimulation in the EV-treated compared with the Hand2-treated mice. However, this effect was more pronounced in response to muscle activation through the nerve. These data indicate that in addition to muscle sympathetic innervation, very old age impairs motor innervation and NMJ transmission, but Hand2 expression in SNs rescues them significantly.

Heart and neural crest derivative 2 expression ameliorates skeletal muscle denervation

We found that SN Hand2 enhances spontaneous and evoked NMJ transmission and attenuates myofibre sympathetic and motor denervation in old mice.¹⁵ Ablation of skeletal muscle sympathetic innervation alters NMJ transmission. Decreased MEPP amplitude and frequency, and decreased EPP amplitude and quantal content,¹² are consistent with a decline in the compound muscle action potential and its rescue by sympathomimetics agents.⁸ Moreover, the Hand2-associated preserved levels in membrane and total AChR are consistent with our previous report that muscle sympathetic innervation regulates the receptor's stability.^{12,15} The expression of pre-synaptic AR reported here can explain how sustained muscle sympathetic innervation enhances NMJ transmission¹⁵ because SN regulation of motoneuron synaptic vesicle release, mediated by β 1-AR and α 2B-AR, is blunted in geriatric mice.^{12,18} Although we have not directly measured NMJ transmission in this study, *Figure 4* shows that maximal tetanic force was sustained, and the response at increasing nerve stimulation frequencies was better preserved in Hand2-treated than EV-treated mice; these processes require maintenance of NMJ transmission.

Skeletal muscle sympathetic innervation is better preserved in the Hand2 group than the EV group as shown by (i) higher TH levels in nerve and muscle, detected by immunoblot; (ii) a longer muscle sympathetic axon path; and (iii) a shorter distance between SNs and NMJs, confirmed by immunohistochemistry. NMJ preterminal and post-terminal colocalization and quantification of NF path length per muscle area show that preserving sympathetic innervation enhances myofibre motor innervation. The mechanism underlying preservation of muscle sympathetic and motor innervation is uncertain; however, low PP2A and PP1 phosphatase levels and more NFH-subunit, NFM-subunit, and NFL-subunit phosphorylation indicate that NF phosphorylation plays a role in stabilizing muscle motor innervation in Hand2-treated mice. This conclusion is supported by the analysis of old mice,¹⁵ and previous confocal and electron microscopy studies on muscle sympathetic ablation, which show compromised NF phosphorylation and disorganized axon NF and microtubules.¹²

Hand2 up-regulates the genes encoding critical components of NMJ and myofibre innervation, as defined by

Ingenuity Pathway Analysis, which shows that synaptogenesis signalling is a primary pathway ($P = 4.52e - 03$). Hand2 also up-regulates the *clf1/cmklr1*, *nrxn2*, *efna2*, and *arrb2*, which play roles in cellular inflammation, inflammatory pain perception, cell proliferation, and β -AR activity, respectively. Down-regulation of the *cytokine receptor-like factor 1 (clf1)* and *chemokine-like receptor 1 (cmklr1)* genes prevents SNS stimulation, leading to higher systemic blood pressure and dysregulated sympathetic and motor neuron transmission. Both genes were down-regulated at an earlier mouse age (22 months),¹⁵ but these studies, like ours, indicate that Hand2 plays a role in SNS-mediated inflammation and immune system function.

Sustained sympathetic neuron heart and neural crest derivative 2 expression prevents activation of the myofibre $G\alpha_{i2}$ -Hdac4-myogenin-MyoD-atrogin/MuRF1 signalling cascade and PKA modifications associated with ageing

The models of muscle sympathetic ablation and induced Hand2 expression in old age show down-regulation of $G\alpha_{i2}$, which activates the Hdac4-myogenin-MyoD cascade to raise MuRF1 levels and preserve AChR stability.^{12,15} We found that Hand2 expression in SNs prevents the decrease in $G\alpha_{i2}$ levels with very old age and averts this signalling cascade, which has been associated with muscle motor denervation.²⁷ Specifically, it lowers Hdac4 concentration to improve motor axon function²⁸ and down-regulates myogenin and myoD,¹⁵ both associated with muscle denervation, in GA and TA muscles. Note that down-regulating this signalling cascade reduces atrogins. MuRF1 is expressed in both type I and type II fibres, but predominantly the latter; it is highly enriched in the post-terminal, interacts with AChR in endocytic structures,²⁹ and participates in muscle trophism and maintenance.³⁰ In sympathectomized MuRF1KO mice, AChR is partitioned between the sarcolemma and subsarcolemmal domain, as it is in innervated young mice.⁹ Consistently, Hand2-induced preservation of muscle sympathetic innervation down-regulates both MuRF1 and atrogin and prevents AChR endocytosis.

In old mice, the PKA RI α subunit is largely removed from the NMJ—while PKA RII α and RII β are enriched there.¹⁶ Here, we found that SN Hand2, like other interventions to counter muscle denervation,¹⁶ up-regulates PKA RI in the TA muscle and down-regulates PKA RII and the PKA RII/PKA RI ratio in both GA and TA muscles at very old age.

Mechanisms that attenuate age-related decline in muscle mass and ex vivo force/in vivo strength

Hand2 treatment preserves muscle Akt phosphorylation, a critical step in the activation of the non-canonical β -AR

pathway, which leads to FoXO1 phosphorylation and MuRF1 and atrogin/MAFbx exclusion from the nucleus and down-regulation. This mechanism, together with down-regulation of the Hdac4-myogenin-MyoD-atrogin/MuRF1 signalling cascade (see earlier), reduces atrogin expression to attenuate muscle atrophy.³¹ Although protein synthesis increases in unperturbed aged muscles,³² decreased muscle protein synthesis, increased protein breakdown, and blunted stimulation of muscle protein synthesis rates to common anabolic stimuli in skeletal muscle tissue or a combination of these factors have been reported in sarcopenia.³³ MuRF1 and MAFbx are up-regulated in ageing humans and rodents.³³ However, we acknowledge that not measuring protein synthesis and degradation is a limitation of the study.

Hand2 also decreases I κ B and NF- κ B phosphorylation. Although our analysis of muscle inflammation in Hand2-treated and EV-treated geriatric mice is not yet exhaustive, we show that long-term, induced expression of Hand2 in peripheral SNs leads to a significant down-regulation of inflammation markers. NF- κ B signalling plays a role in geriatric mouse skeletal muscle atrophy.³⁴ These results support our RNA-sequencing analysis showing that Hand2-induced *clf1* and *cmklr1* down-regulation decreases I κ B activation, leading to nuclear exclusion of NF- κ B and preventing activation of the canonical pro-inflammatory pathway. Cytokines down-regulate *Hand2* in cultured SNs, while Hand2 overexpression rescues the noradrenergic phenotype. These observations support a third mechanism, in addition to reduced levels of PKA RI¹⁶ and Hand2 genomic DNA hypermethylation, for decreased *Hand2* transcription with ageing.¹⁵

Rapamycin-induced mTORC1 inhibition prevents age-related muscle loss, while its chronic activation advances muscle damage and loss, inhibiting constitutive and starvation-induced autophagy in skeletal muscle.³⁵ We found that in both GA and TA muscles, Hand2 treatment sustains mTORC1 phosphorylation at serine 2448, fine-tuning its activity at the 'repressor domain',³⁶ in old,¹⁵ and, here, very old age. Deleting this site strongly activates mTORC1. Increased phosphorylation at the repressor domain prevents ULK and ATG13 phosphorylation, activating autophagy.

One common feature of all age-related changes at the tissue level is the accumulation of damage and harmful modifications in DNA, proteins, lipids, and cellular organelles; autophagic efficiency declines over time, and intracellular waste products accumulate.³⁴ Robust genetic evidence across species supports the inhibition of autophagy with ageing^{37,38}; Hand2 restores it in old mice,¹⁵ but the effect on very old mice is unknown. Analysis of muscle autophagy showed lower p62 and higher ATG-7 levels and LC3-I lipidation in the Hand2 group than in EV group. Atg7 ablation induces NMJ degeneration and precocious ageing,³⁸ which suggests that high ATG-7 levels are required to improve muscle autophagy. Autophagy selectively degrades the LC3-binding adaptor p62 protein [sequestosome-1 (SQSTM1)], and because a drop in p62 is

associated with activation of the autophagic process, it serves as a readout of autophagic flux, together with LC3-I conversion to LC3-II. Non-significant changes in heat shock cognate 71 kDa protein levels indicate that sustained Hand2 expression in SNs activates macroautophagy, but not CMA, in old age. Note that direct stimulation of SNs activates muscle post-synaptic β 2-AR, cAMP production, and import of the transcriptional co-activator peroxisome proliferator-activated receptor γ -coactivator 1 α into the myonucleus,⁸ which increases autophagy.

Hand2 treatment significantly up-regulates *Smad1*, an important upstream regulator (P -value = $8.39e^{-5}$) that mediates the BMPs involved in a range of biological activities, including cell growth, apoptosis, morphogenesis, development, and immune responses

In summary, the SNS regulates many primary synaptic and non-synaptic events. Inducing Hand2 expression in peripheral SNs from middle-aged mice improves myofibre innervation, muscle mass, and function maintenance well into very old age (Figure 8).

Acknowledgements

The authors of this manuscript certify that they comply with the ethical guidelines for authorship and publishing in the *Journal of Cachexia, Sarcopenia and Muscle*.⁴⁰

Conflict of interest

None declared.

Funding

This research was supported by the National Institutes of Health Grants R01AG057013 and R01AG057013-02S1 to O. D. and the Claude D. Pepper Older Americans Independence Center at Wake Forest School of Medicine (P30-AG21332) and the Wake Forest Comprehensive Cancer Center (P30CA012197).

Online supplementary material

Additional supporting information may be found online in the Supporting Information section at the end of the article.

Figure S1. Hand-2 treatment preserves muscle weight and strength in aged mice. Compared to EV-treatment, Hand2 significantly increased tibialis anterior (TA) (A), gastrocnemius (GA) (B), extensor digitorum longus (EDL) (C), and soleus (D)

muscle, but not body (E), heart (F), or visceral fat (G) weight. We used 10 muscles from 10 EV-treated mice and 8 muscles from 10 Hand2-treated mice to count TA, GA, EDL, and soleus muscles and measure visceral fat; 10 hearts per group to measure their weight; and 10 mice per group to measure body weight. We used nonpaired t-tests for group comparisons except for treadmill data where we applied the ANOVA repeated measures test.

Figure S2. Mobility, tested in the open arena setting, did not differ between groups in terms of spontaneous maximum speed (H), average speed (I), total distance traveled (J), time spent in motion (K), or treadmill running time (M), but net hanging time (L) was significantly longer in the Hand2- than EV-treated mice. We used 6 mice per group to assess spontaneous mobility and body strength. Nonpaired t-tests were used for group comparisons.

Figure S3. Sympathetic neuron Hand2 preserves NF phosphorylation. The Hand2 group has significantly more sciatic-peroneal (SP) nerve phospho-NFH (A), phospho-NFM (B), and phospho-NFL (C) than the EV group. Phosphatases PP2A (D) and PP1 (E) declined with sympathetic neuron Hand2 expression. Data were statistically analyzed using a nonpaired t-test.

Figure S4. Sustained sympathetic neuron Hand2 expression prevents activation of atrogenes. GA and TA muscles $G\alpha_{12}$ (A), HDAC4 (D), myogenin (G), MyoD (J), atrogenin (M), and MuRF1 (P) levels, analyzed by immunoblot. The digital optical density of the bands normalized to GAPDH is represented in B-C, E-F, H-I, K-L, N-O, and Q-R, respectively. $N = 8$ GA or TA muscles from 8 different mice per treatment group. Data were statistically analyzed using a nonpaired t-test.

Figure S5. Sympathetic neuron Hand2 sustains muscle PKA RI and Akt phosphorylation levels in geriatric mice. Hand2 treatment sustained TA muscle PKA RI (A, B), but not PKA RII (C, D) or the PKA RII/PKA RI ratio (E). Hand2 treatment sustained phospho-Akt/total-Akt in both muscles (F), as quantified in G. $N = 8$ GA or TA muscles from 8 different mice per treatment group. Data were statistically analyzed using a nonpaired t-test.

Figure S6. Sympathetic neuron Hand2 regulates phosphorylation of key components of gene transcription, cell signaling, and inflammation. Hand2 treatment sustains mTORC1 phosphorylation (A, B) and FoXO1 (C, D), while decreasing FoXO3 in the TA (E, F) and NF κ B (G, H) and I κ B (I, J) phosphorylation in both GA and TA muscles. $N = 8$ GA or TA muscles from 8 different mice per treatment group. Data were statistically analyzed using a nonpaired t-test.

Figure S7. Sympathetic neuron Hand2 maintains skeletal muscle macroautophagy flux, but not CMA in geriatric mice. Hand2-treated mice show less p62 (A-B), a higher LC3-II/LC3-I ratio (C, D), and more Atg7 (E, F) in both GA and TA muscles than the EV group. Lamp2 (G, H) and HSC70 (I, J) levels did not differ significantly between groups. $N = 6$ GA

or TA muscles from 6 different mice per treatment group. Data were statistically analyzed using a nonpaired t-test.

Figure S8. Original Immunoblots for Figures 3 and 6 and Supplementary Figures 1–7.

Table S1. Antibodies used for immunoblot and immunohistochemistry.

Table S2. Differentially expressed genes in Hand2- and EV-treated mice analyzed by RNA-seq. This spreadsheet shows RNA-seq data collected from 4 Hand2- and 3 EV-treated mice.

References

- Larsson L, Degens H, Li M, Salviati L, Yi L, Thompson W, et al. Sarcopenia: aging-related loss of muscle mass and function. *Physiol Rev* 2019;**99**:427–511.
- Wang ZM, Zheng Z, Messi ML, Delbono O. Extension and magnitude of denervation in skeletal muscle from ageing mice. *J Physiol* 2005;**565**:757–764.
- Delbono O. Neural control of aging skeletal muscle. *Aging Cell* 2003;**2**:21–29.
- Hunter GR, McCarthy JP, Bamman MM. Effects of resistance training on older adults. *Sports Med* 2004;**34**:329–348.
- Messi ML, Li T, Wang ZM, Marsh AP, Nicklas B, Delbono O. Resistance training enhances skeletal muscle innervation without modifying the number of satellite cells or their myofiber association in obese older adults. *J Gerontol A Biol Sci Med Sci* 2016;**71**:1273–1280.
- Delbono O, Rodrigues ACZ, Bonilla HJ, Messi ML. The emerging role of the sympathetic nervous system in skeletal muscle motor innervation and sarcopenia. *Ageing Res Rev* 2021;**67**:101305.
- Lipsitz LA, Novak V. *Aging and Autonomic Function*, 3rd ed. Rochester: Mayo Foundation; 2008.
- Khan MM, Lustrino D, Silveira WA, Wild F, Straka T, Issop Y, et al. Sympathetic innervation controls homeostasis of neuromuscular junctions in health and disease. *Proc Natl Acad Sci U S A* 2016;**113**:746–750.
- Rodrigues ACZ, Messi ML, Wang Z-M, Abba MC, Pereyra A, Birbrair A, et al. The sympathetic nervous system regulates skeletal muscle motor innervation and acetylcholine receptor stability. *Acta Physiol* 2018;**225**:e13195.
- Lynch GS, Ryall JG. Role of β -adrenoceptor signaling in skeletal muscle: implications for muscle wasting and disease. *Physiol Rev* 2008;**88**:729–767.
- Baker DJ, Constantin-Teodosiu D, Jones SW, Timmons JA, Greenhaff PL. Chronic treatment with the β_2 -adrenoceptor agonist prodrug BRL-47672 impairs rat skeletal muscle function by inducing a comprehensive shift to a faster muscle phenotype. *J Pharmacol Exp Ther* 2006;**319**:439–446.
- Rodrigues AZC, Wang Z-M, Messi ML, Delbono O. Sympathomimetics regulate neuromuscular junction transmission through TRPV1, P/Q- and N-type Ca^{2+} channels. *Mol Cell Neurosci* 2019;**95**:59–70.
- Stanzel S, Stubbusch J, Pataskar A, Howard MJ, Deller T, Ernsberger U, et al. Distinct roles of Hand2 in developing and adult autonomic neurons. *Dev Neurobiol* 2016;**76**:1111–1124.
- Flurkey K, Currer JM, Harrison DE. In Fox JG, ed. *The Mouse in Aging Research*. Boston: Elsevier; 2007. p 637–672.
- Rodrigues ACZ, Wang Z-M, Messi ML, Bonilla HJ, Liu L, Freeman WM, et al. Heart and neural crest derivative 2-induced preservation of sympathetic neurons attenuates sarcopenia with aging. *J Cachexia Sarcopenia Muscle* 2020;**12**:91–108.
- Xu Z, Feng X, Dong J, Wang Z-M, Lee J, Furdai C, et al. Cardiac troponin T and fast skeletal muscle denervation in ageing. *J Cachexia Sarcopenia Muscle* 2017;**8**:808–823.
- Wang Z-M, Rodrigues ACZ, Messi ML, Delbono O. Aging blunts sympathetic neuron regulation of motoneurons synaptic vesicle release mediated by β_1 - and α_2B -adrenergic receptors in geriatric mice. *J Gerontol A Biol Sci Med Sci* 2020;**75**:1473–1480.
- Wang ZM, Messi ML, Grinevich V, Budygin E, Delbono O. Postganglionic sympathetic neurons, but not locus coeruleus optostimulation, activates neuromuscular transmission in the adult mouse in vivo. *Mol Cell Neurosci* 2020;**109**:103563.
- Papa S, Zazzeroni F, Bubici C, Jayawardena S, Alvarez K, Matsuda S, et al. Gadd45 β mediates the NF- κ B suppression of JNK signaling by targeting MKK7/JNK2. *Nat Cell Biol* 2004;**6**:146–153.
- Wilkie TM, Gilbert DJ, Olsen AS, Chen XN, Amatruda TT, Korenberg JR, et al. Evolution of the mammalian G protein α subunit multigene family. *Nat Genet* 1992;**1**:85–91.
- Tsarovina K, Reiff T, Stubbusch J, Kurek D, Grosveld FG, Parlato R, et al. The Gata3 transcription factor is required for the survival of embryonic and adult sympathetic neurons. *J Neurosci* 2010;**30**:10833–10843.
- Hendershot TJ, Liu H, Clouthier DE, Shepherd IT, Coppola E, Studer M, et al. Conditional deletion of Hand2 reveals critical functions in neurogenesis and cell type-specific gene expression for development of neural crest-derived noradrenergic sympathetic ganglion neurons. *Dev Biol* 2008;**319**:179–191.
- Jones A, Teschendorff AE, Li Q, Hayward JD, Kannan A, Mould T, et al. Role of DNA methylation and epigenetic silencing of *HAND2* in endometrial cancer development. *PLoS Med* 2013;**10**:e1001551.
- Zheng Z, Wang ZM, Delbono O. Insulin-like growth factor-1 increases skeletal muscle DHP α 1S transcriptional activity by acting on the cAMP-response element-binding protein element of the promoter region. *J Biol Chem* 2002;**277**:50535–50542.
- Rauen T, Hedrich CM, Tenbrock K, Tsokos GC. cAMP responsive element modulator: a critical regulator of cytokine production. *Trends Mol Med* 2013;**19**:262–269.
- Alley DE, Metter EJ, Griswold ME, Harris TB, Simonsick EM, Longo DL, et al. Changes in weight at the end of life: characterizing weight loss by time to death in a cohort study of older men. *Am J Epidemiol* 2010;**172**:558–565.
- Minetti GC, Feige JN, Bombard F, Heier A, Morvan F, Nürnberg B, et al. Gai2 signaling is required for skeletal muscle growth, regeneration, and satellite cell proliferation and differentiation. *Mol Cell Biol* 2014;**34**:619–630.
- Moresi V, Williams AH, Meadows E, Flynn JM, Potthoff MJ, McAnally J, et al. Myogenin and class II HDACs control neurogenic muscle atrophy by inducing E3 ubiquitin ligases. *Cell* 2010;**143**:35–45.
- Rudolf R, Bogomolovas J, Strack S, Choi KR, Khan MM, Wagner A, et al. Regulation of nicotinic acetylcholine receptor turnover by MuRF1 connects muscle activity to endo/lysosomal and atrophy pathways. *Age (Dordr)* 2013;**35**:1663–1674.
- Moriscot AS, Baptista IL, Bogomolovas J, Witt C, Hirner S, Granzier H, et al. MuRF1 is a muscle fiber-type II associated factor and together with MuRF2 regulates type-II fiber trophicity and maintenance. *J Struct Biol* 2010;**170**:344–353.
- Ryall JG, Schertzer JD, Alabakis TM, Gehrig SM, Plant DR, Lynch GS. Intramuscular β_2 -agonist administration enhances early regeneration and functional repair in rat skeletal muscle after myotoxic injury. *J Appl Physiol* 2008;**105**:165–172.
- Miller BF, Baehr LM, Musci RV, Reid JJ, Peeler FF 3rd, Hamilton KL, et al. Muscle-specific changes in protein synthesis with aging and reloading after disuse atrophy. *J Cachexia Sarcopenia Muscle* 2019;**10**:1195–1209.

33. Altun M, Besche HC, Overkleeft HS, Piccirillo R, Edelmann MJ, Kessler BM, et al. Muscle wasting in aged, sarcopenic rats is associated with enhanced activity of the ubiquitin proteasome pathway. *J Biol Chem* 2010;**285**:39597–39608.
34. Salminen AL, Brandt A, Samuelsson K, Toytari O, Malmivaara A. Mobility devices to promote activity and participation: a systematic review. *J Rehabil Med* 2009;**41**: 697–706.
35. Castets P, Lin S, Rion N, Fulvio S, Romanino K, Guridi M. Sustained activation of mTORC1 in skeletal muscle inhibits constitutive and starvation-induced autophagy and causes a severe, late-onset myopathy. *Cell Metab* 2013;**17**:731–744.
36. Figueiredo VC, Markworth JF, Cameron-Smith D. Considerations on mTOR regulation at serine 2448: implications for muscle metabolism studies. *Cell Mol Life Sci* 2017;**74**:2537–2545.
37. Rubinsztein DC, Marino G, Kroemer G. Autophagy and aging. *Cell* 2011;**146**: 682–695.
38. Carnio S, LoVerso F, Baraibar Martin A, Longa E, Khan Muzamil M, Maffei M, et al. Autophagy impairment in muscle induces neuromuscular junction degeneration and precocious aging. *Cell Rep* 2014;**8**: 1509–1521.
39. Li Y, Lee Y, Thompson WJ. Changes in aging mouse neuromuscular junctions are explained by degeneration and regeneration of muscle fiber segments at the synapse. *J Neurosci* 2011;**31**:14910–14919.
40. von Haehling S, Morley JE, Coats AJS, Anker SD. Ethical guidelines for publishing in the Journal of Cachexia, Sarcopenia and Muscle: update 2019. *J Cachexia Sarcopenia Muscle* 2019;**10**:1143–1145.